*International Journal of Automotive Technology*, Vol. 5, No. 2, pp. 123–133 (2004)


1229-9138/2004/016-07

# WHEEL SLIP CONTROL WITH MOVING SLIDING SURFACE FOR TRACTION CONTROL SYSTEM

K. CHUN[1] and M. SUNWOO[2]*

[1]ACE Lab, Hanyang University, Seoul 133-791, Korea
[2]Department of Automotive Engineering, Hanyang University, Seoul 133-791, Korea

*(Received 29 November 2003; Revised 11 February 2004)*

**ABSTRACT**–This paper describes a robust and fast wheel slip tracking control using a moving sliding surface technique. A traction control system (TCS) is the active safety system used to prevent the wheel slipping and thus improve acceleration performance, stability and steerability on slippery roads through the engine torque and/or brake torque control. This paper presents a wheel slip control for TCS through the engine torque control. The proposed controller can track a reference input wheel slip in a predetermined time. The design strategy investigated is based on a moving sliding surface that only contains the error between the reference input wheel slip and the actual wheel slip. The used moving sliding mode was originally designed to ensure that the states remain on a sliding surface, thereby achieving robustness and eliminating chattering. The improved robustness in driving is important due to changes, such as from dry road to wet road or vice versa which always happen in working conditions. Simulations are performed to demonstrate the effectiveness of the proposed moving sliding mode controller.

**KEY WORDS :** TCS, Slip control, Moving sliding surface

## 1. INTRODUCTION

Recently, TCS has been receiving a lot of attracting attention because it maintains the traction ability and steerability of vehicles on low-$\mu$ surface roads by controlling the slip rate between the tire and road surface. On a slippery road surface, the acceleration process of a vehicle often leads to wheel spin. The friction coefficient between the tire and the road will reduce further with increasing wheel slip.

The objective of antislip control (or traction control system) is to determine the maximum effective engine torque that can be transmitted to the drive wheels so that the level of tractive slip remains within a stable range. The control of wheel slip requires that the torque delivered by the engine be distributed optimally to the drive wheels.

With the introduction of vehicle dynamics control, an operating point may not necessarily be at the peak of the $\mu$-$\lambda$ curve. In fact, it could be at a point that is in the traditionally unstable region of the $\mu$-$\lambda$ curve. The main difficulty arising in the design of a wheel slip control is due to the strong nonlinearity and uncertainty in the problem. Sliding mode control is a preferable approach for this kind of problem; due to changes which always happen in working conditions, the robustness of sliding mode control is an advantage. Sliding mode controllers have been designed previously for the purpose of controlling wheel slip (Drakunov *et al.*, 1995; Kazemi *et al.*, 2000; Ünsal and Kachroo, 1999; Kueon and Bedi, 1999; El Hadri *et al.*, 2001; Lee and Sin, 2000; Landaluze *et al.*, 1999).

Unlike the conventional sliding mode, sliding mode control with a moving sliding surface has a robust and fast response. This method keeps the sliding mode from the initial state and thus improves robustness. Reduced reaching control input improves the chattering problem, too (Choi and Park, 1994; Choi *et al.*, 1994; Bartoszewicz, 1995; Choi and Kim, 1997; Ha *et al.*, 1999).

This paper proposes a robust wheel slip control with a specified time for traction control system. Using the moving sliding surface technique, robustness and chattering are improved. The proposed design method is simple and the designer can determine a reaching time. The stability is proved by the Lyapunov technique. The proposed scheme is evaluated by computer simulation with an 8 DOF vehicle model and a nonlinear tire model. The results indicate that the noble sliding technique improves vehicle's stability and steerability.

*Corresponding author. e-mail: msunwoo@hanyang.ac.kr

## 2. DYNAMICS MODEL

In this paper, we develop a new TCS based on the moving sliding surface control method. The slip of the drive wheels is controlled to prevent the skidding of wheels and to obtain maximum tractive force.

### 2.1. Vehicle Dynamics

It is assumed that the following sensor information is available: wheel speed, $\omega$, at each corner, longitudinal accelerometers, $a_x$, per axle lateral accelerometers, $a_y$, and a yaw rate sensor, $r$, at the center of gravity of the vehicle. Also, tire force sensors or observers are assumed to be present. Figure 1 and Figure 2 show the layout of the variables for the vehicle and the wheel dynamics, respectively.

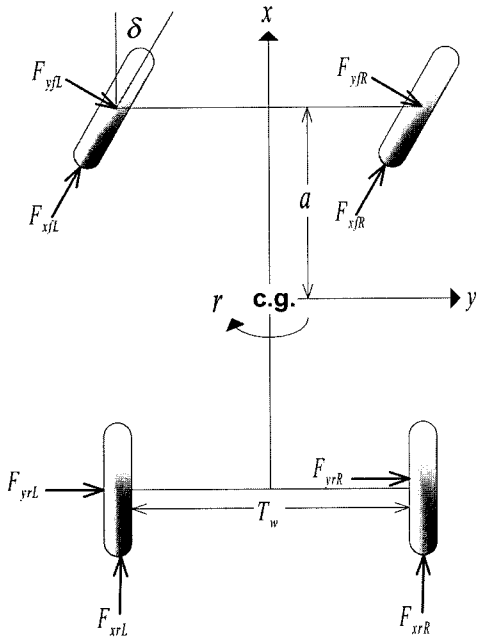


Figure 1. Vehicle dynamics layout.

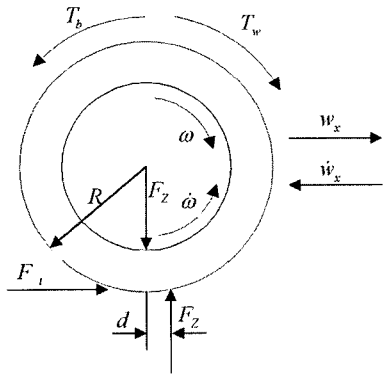


Figure 2. Wheel dynamics layout.

In formulating the wheel slip, $\lambda$, control problem, the wheel acceleration, $\dot{\omega}$, is needed. The wheel acceleration, $\dot{\omega}$, is calculated by

$$I_w\dot{\omega}=T_t-T_b \tag{1}$$

where $T_t$ is the tire tractive torque, and $T_b$ is the brake torque applied to the wheel and assumed to be zero because TCS is done by the engine torque control. Equation (1) can be expanded to

$$I_w\dot{\omega}=T_{wt}-RF_x-dF_z-T_b \tag{2}$$

where $I_w$ is the mass moment inertia of the wheel about the axis of rotation, $T_{wt}$ is the wheel torque, $F_z$ is the wheel normal force, $R$ is the wheel radius and $d$ is the distance between the spin axis and the road reaction vertical force. During wheel acceleration, $F_x>0$. For simulation purposes, the longitudinal (tractive) tire force, $F_x$, is modeled using a Pacjeka tire model (Pacjeka and Bakker, 1990).

### 2.2. Engine Model

The engine model used in this paper is from Yoon and Sunwoo (1999). As shown in Figure 3, this is a three-state model: intake manifold pressure, engine speed, and fuel mass in the fuel film. The time constants of mass airflow through the throttle body and torque production model are relatively smaller than three state variables, so they are expressed as algebraic relations.

The flow of air through a throttle valve can be considered as a special case of the isentropic flow of compressible fluid (Hendricks and Sorenson, 1990). When the following simple form is applied to the actual engine controller, the normalized functions *TC* and *PRI* can be put into look-up tables, which can be accessed quickly and easily.

$$\dot{m}_{at}=C_D\cdot MA\cdot TC\cdot PRI \tag{3}$$

*MA* is the maximum possible flow rate through the specific throttle, and *TC* is a normalized flow as a function of the cross-sectional area, and *PRI* is a normalized flow as a function of pressure ratio. These are as follows:

$$MA=\frac{P_{amb}A_{th}(\alpha_{\max})}{\sqrt{RT_{amb}}} \tag{4}$$

$$TC=\frac{A_{th}(\alpha)}{A_{th}(\alpha_{\max})} \tag{5}$$

$$PRI=P_R^{\frac{1}{\gamma}}\left(\frac{2}{\gamma+1}\right)^{\frac{\gamma+1}{2(1-\gamma)}}\left\{\frac{2}{\gamma-1}\left[1-P_R^{\frac{1}{\gamma}}\right]\right\}^{\frac{1}{2}},\ \text{if } P_R\geq P_{CR} \tag{6}$$

$$PRI=1.0 \qquad \text{otherwise}$$

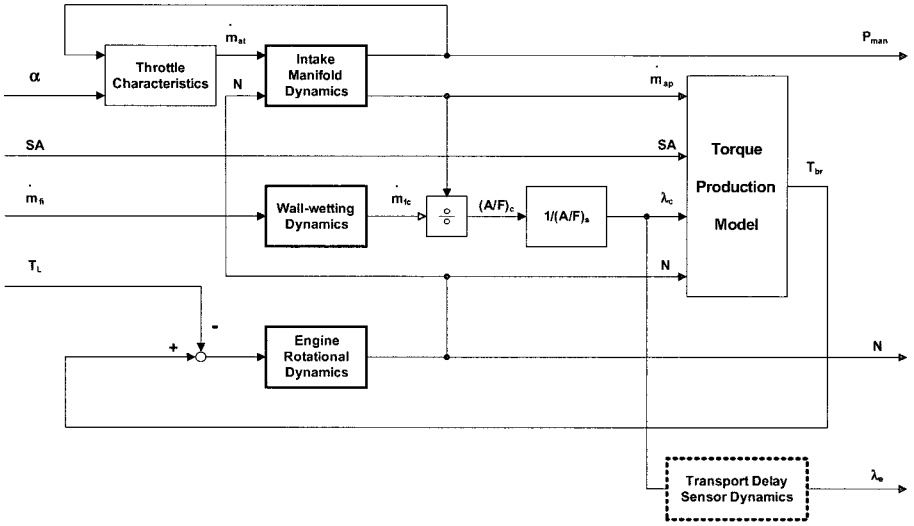


Figure 3. Block diagram of three-state dynamic engine model.

$$P_R=\frac{P_T}{P_0}\approx\frac{P_m}{P_{amb}},\quad P_{CR}=\left(\frac{2}{\gamma+1}\right)^{\frac{\gamma}{\gamma+1}} \tag{7}$$

The discharge (or flow) coefficient, $C_D$ is a function of the throttle angle (i.e., throttle geometry) and the pressure ratio across the throttle body. $P_{amb}$ is the ambient pressure and $T_{amb}$ is the ambient temperature. $\gamma$ is the specific heat ratio.

If the shape of the throttle bore is assumed to be circular and the projection area of the throttle plate about the vertical plane is ellipsoidal, the cross-sectional area of throttle opening, $A_{th}(\alpha)$ is represented by equation (8)

$$\begin{aligned}A_{th}(\alpha)=&\frac{\pi}{4}D^2\left(1-\frac{\cos\alpha}{\cos\alpha_0}\right)+\frac{D^2}{2}\sin^{-1}\left(\frac{d}{D}\right)\\&-\frac{d}{2}\sqrt{D^2-d^2}+\frac{D^2\cos\alpha}{2\cos\alpha_0}\sin^{-1}\left(\frac{d\cos\alpha_0}{D\cos\alpha}\right)\\&+\frac{d}{2\cos\alpha}\sqrt{D^2\cos^2\alpha-d^2\cos^2\alpha_0}\end{aligned} \tag{8}$$

For the derivation of the manifold pressure state equation, the conservation of air mass in the intake manifold, equation (9), and the differential form of the ideal gas law, equation (10) are used.

$$\dot{m}_{ai}=\dot{m}_{at}-\dot{m}_{ap} \tag{9}$$

$$\dot{m}_{ai}=\frac{d}{dt}\left(\frac{P_mV_m}{RT_m}\right) \tag{10}$$

Substituting equation (10) into equation (9), the manifold pressure state equation, (11) is obtained.

$$\dot{P}_m=\frac{RT_m}{V_m}(\dot{m}_{at}-\dot{m}_{ap})+P_m\left(\frac{\dot{T}_m}{T_m}\right)\approx\frac{RT_m}{V_m}(\dot{m}_{at}-\dot{m}_{ap}) \tag{11}$$

The mass airflow out of the intake manifold is represented by a well-known speed-density algorithm. In a four stroke, four cylinder engine, this relationship can be written as:

$$\dot{m}_{ap}=\frac{V_D}{120RT_m}\eta_{vol}P_mN \tag{12}$$

where $V_D$ is the displacement volume of engine, $\eta_{vol}$ is the volumetric efficiency, $N$ is the engine speed[rpm], $R$ is the gas constant and $T_m$ is the intake manifold air temperature. An intake manifold pressure state equation, (13), can be obtained by substituting equation (12) into equation (11).

$$\begin{aligned}\frac{dP_m}{at}=&-\frac{V_D\eta_{vol}N}{120V_m}P_m+\frac{RT_m}{V_m}\dot{m}_{at}(\alpha,P_m)\\=&-\frac{1}{\tau_m}(P_m-P_{m,ss})\end{aligned} \tag{13}$$

where $V_m$ is the volume of intake manifold and surge tank, $\tau_m$ corresponds to the time constant of the intake manifold pressure state equation represented by the first order differential equation, and $P_{m,ss}$ is the manifold pressure determined from the throttle angle and engine speed at a steady state.

$$\tau_m=\frac{120V_m}{V_D\eta_{vol}N},\quad P_{m,ss}=\frac{120RT}{V_D\eta_{vol}N}\dot{m}_{ai} \tag{14}$$

It is possible to convert the intake manifold pressure state equation into an air charge per stroke equation (Powell *et al.*, 1998) by multiplying $(V_D\eta_{vol}/4RT_m)$ to both sides of equation (13). This form of the equation is very useful in the application of model-based AFR control because the computational burden can be substantially reduced.

$$\dot{m}_{ac}=-\frac{1}{\tau_m}(m_{ac}-m_{ac,ss}) \tag{15}$$

where $m_{ac,ss}$ is the steady state air charge per stroke, and can be obtained from the steady state engine test.

$$m_{ac,ss}=\frac{30}{N}\dot{m}_{at} \tag{16}$$

The characteristics of the fuel injection process are very complex and are largely influenced by various factors, such as injection schemes, spray patterns, injection timing, port geometry, intake manifold wall temperature, fuel rail pressure, and other factors. However, it is actually not easy to implement such complicated fuel delivery models which consider all aspects mentioned above to the real time engine control applications.

It is assumed that the fuel to be injected is proportional to the airflow, and that some fraction ($X$) of that impacts the intake manifold walls and forms a fuel puddle on the walls. It is also assumed that fuel leaves a film in proportion to the amount of fuel in the film. The continuity equation for the fuel film can be written as (Aquino, 1981).

$$\dot{m}_{ff}=-\frac{1}{\tau_f}m_{ff}+X\dot{m}_{fi} \tag{17}$$

The fraction of fuel, which does not form fuel film, directly enters the cylinder with airflow is represented by equation (18).

$$\dot{m}_{fv}=(1-X)\dot{m}_{fi} \tag{18}$$

Thus, the actual fuel flow rate, which enters the cylinder, is the sum of $\dot{m}_{fv}$ and the evaporated fuel from the film with the time constant $\tau_f$.

$$\dot{m}_{fc}=\dot{m}_{fv}+\frac{1}{\tau_f}m_{ff} \tag{19}$$

where $\dot{m}_{fi}$ is the injected fuel flow rate from the injector.

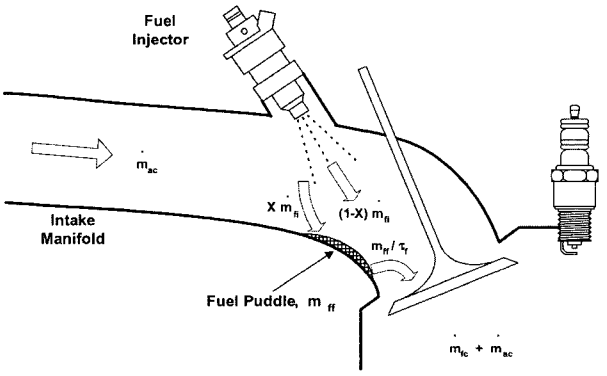


Figure 4. Schematic diagram of fuel transport process in PFI engine.

Therefore, the actual AFR in the cylinder is given by $\dot{m}_{ac}/\dot{m}_{fc}$, and it can also be represented by an equivalence ratio ($\phi_c=1/\lambda$).

$$\phi_c(t)=(A/F)_s\frac{\dot{m}_{fc}(t)}{\dot{m}_{ac}(t)} \tag{20}$$

Figure 4 represents the schematic diagram of fuel transport process in the intake manifold.

In order to understand the dynamic charactereistics of AFR with the variation of important fuel delivery model parameters ($X$ and $\tau_f$), the transient response of AFR with step fuel perturbation is predicted. If equation (17) is regarded as a kind of an initial value problem, the solution is given by

$$m_{ff}(t)=e^{-\frac{1}{\tau_f}}\tau_f X\dot{m}_{fi}(0)+\tau_f X\dot{m}_{fi}(t)\left(1-e^{-\frac{1}{\tau_f}}\right) \tag{21}$$

where $\dot{m}_{fi}(t)$ =constant at step test, and
$m_{ff}(0)=\tau_f X\dot{m}_{fi}(0)$ at steady state

Therefore, fuel flow rate into the cylinder is

$$\begin{aligned}\dot{m}_{fc}(t)&=(1-X)\dot{m}_{fi}(t)+\frac{1}{\tau_f}m_{ff}(t)\\&=\dot{m}_{fi}(t)-X\Delta\dot{m}_{fi}(t)e^{-\frac{1}{\tau_f}}\end{aligned} \tag{22}$$

where $\Delta\dot{m}_{fi}(t)=\dot{m}_{fi}(t)-\dot{m}_{fi}(0)$
If the throttle angle is assumed to be constant and only step fuel perturbation is applied, the equivalence ratio in the cylinder is represented by equation (23).

$$\phi_c(t)=\frac{(A/F)_S}{\dot{m}_{ac}(t)}\left[\dot{m}_{fi}(t)-X\Delta\dot{m}_{fi}(t)e^{-\frac{1}{\tau_f}}\right] \tag{23}$$

The combustion process in the cylinder produces engine torque, and the quantity of the torque produced is influenced by the AFR of the mixture in the cylinder, spark timing, and combustion efficiency. The transport delay with respect to each engine event gives dynamic characteristics to the torque production model.

It is assumed that the dynamic torque of the engine is a function of engine speed, air charge per stroke, spark timing, and the AFR. Under this assumption, the predictive torque production model is derived from the steady state engine experiments. One of the most important things in the development of the torque production model is the identification of the optimal spark timing (MBT) at each of the operating conditions. Most engine models published previously (Dobner, 1983; Moskwa and Hedrick, 1992; Hendricks and Sorenson, 1990) were developed under the assumption that the engine is operated near the stoichiometric AFR only, and they did not consider the change of the MBT with respect to the change of the AFR. Recent advanced engine technologies, such as lean burn, and gasoline direct injection engine, motivate the

development of the engine model, which is applicable to a wide range of AFR.

The MBT at the stoichiometric AFR is identified under various engine speed and load conditions. This is followed by the identification of the MBT at various AFR conditions. The difference between the MBT at the stoichiometric AFR and the MBT at an arbitrary AFR at various engine operating conditions is denoted by $\Delta MBT(\lambda)$. Based upon this approach, the MBT at an arbitrary AFR can be represented by equation (25).

$$(MBT)_{\lambda_s}=f(m_{ac},n)$$
$$=m_o+m_1n+m_2n^2+(m_3+m_4n)m_{ac} \quad (24)$$

$$(MBT)_{\lambda}=(MBT)_{\lambda_s}+\Delta MBT(\lambda) \quad (25)$$

where $\Delta MBT(\lambda)=d_0+d_1\lambda+d_2\lambda^2$
$(MBT)_{\lambda_s}$ : MBT at stoichiometirc AFR
$(MBT)_{\lambda}$ : MBT at arbitrary AFR

Under the assumption of negligible cylinder-by-cylinder engine torque variations, the indicated torque is obtained from the measurement of IMEP of cylinder #1 using a cylinder pressure sensor (Brunt and Emtage, 1996).

$$IMEP=\frac{\sum_{\varphi_k=\varphi_{IBDC}}^{\varphi_{EBDC}}[P_c(\varphi_k)+P_c(\varphi_{k+1})][V_c(\varphi_k)+(-V_c)(\varphi_{k+1})]}{2V_s} \quad (26)$$

$$T_{ind}=\frac{100V_DIMEP}{6.28N_{cyl}} \quad (27)$$

If AFR and spark timing are fixed, the indicated torque of an engine is a function of engine speed and air charge. Therefore, the indicated torque at the MBT and the stoichiometric AFR can be represented by equation (28).

$$(T_{ind})_{MBT,\lambda_s}=t_0+t_1n+t_2n^2+(t_3+t_4n)m_{ac} \quad (28)$$

The indicated torque at an arbitrary engine condition is obtained from equation (28) multiplied by the efficiencies of the spark timing and the AFR which reflect the changed operating conditions.

$$T_{ind}(n, m_{ac}, \eta_{\Delta SA}, \eta_{\lambda})=(T_{ind})_{MBT,\lambda_s}\cdot\eta_{\Delta\Sigma A}\cdot\eta_{\lambda} \quad (29)$$

where $\eta_{\Delta SA}=s_0+s_1(\Delta SA)+s_2(\Delta SA)^2$
$\Delta SA=(MBT)_{\lambda}-SA$
$\eta_{\lambda}=l_0+l_1\lambda+l_2\lambda^2$

Actually, the indicated torque generated by the combustion of an in-cylinder mixture is decreased by both engine friction and pumping loss. The difference between the indicated torque and the friction and pumping loss becomes the brake torque. The friction and pumping torque, $T_{flp}$, is estimated from the difference between the indicated torque measured from the steady state cylinder pressure and the brake torque obtained from an engine dynamometer. It is well known that the friction and pumping loss is a function of the engine speed and intake manifold pressure (Taylor, 1985). As a result, the friction and pumping torque can be approximated by a polynomial of engine speed and air charge.

$$T_{flp}=p_0+p_1n+p_2n^2+(p_3+p_4n)m_{ac} \quad (30)$$

Summarizing the torque production model used in this study, this model has four inputs (engine speed, air charge, fuel flow rate, and spark timing), six submodels approximated by polynomials, and brake torque as an output.

If each event of the engine is concentrated at one instant of time (Dobner, 1983), the useful transport delays used in this engine model are:

Intake to exhaust delay, $\Delta\varphi_{IE}=489^\circ$ (31)
Intake to torque delay, $\Delta\varphi_{IT1}=279^\circ$
Injection to torque delay, $\Delta\varphi_{IT2}=585^\circ$
Spark to torque delay, $\Delta\varphi_{ST}=75^\circ$

The rotational dynamics of an engine are modeled under the assumption of a lumped parameter system with constant inertia. In an actual engine, the effective polar moment of inertia of the crankshaft, connecting rod, piston, and the valve mechanism changes cyclically due to the varying geometry of the slider-crank mechanism. In addition, torsional vibrations occur due to the pressure pulsation from the firing cylinder. However, the objective of the engine model used in this study is the prediction of the mean value of each state variable, and the approximations stated previously can be regarded as reasonable assumptions.

Using Newton's Second Law, the state equation for engine speed is given by:

$$J_{eff}\frac{dN(t)}{dt}=\frac{30}{\pi}(T_{ind}(t)-T_{flp}(t)-T_L(t)) \quad (32)$$

where

$$T_{ind}(t)=(T_{ind})_{MBT,\lambda_s}(t-\Delta t_{IT1})\cdot\eta_{\Delta SA}(t-\Delta t_{SA})\cdot\eta_{\lambda}(t-\Delta t_{IT2})$$

with $\Delta t_{IT1}=\frac{\Delta\varphi_{IT1}}{6N(t)}$, $\Delta t_{IT2}=\frac{\Delta\varphi_{IT2}}{6N(t)}$, $\Delta t_{ST}=\frac{\Delta\varphi_{ST}}{6N(t)}$

### 2.3. Wheel Slip Dynamics

Figure 5 shows the longitudinal (driving) tire force and lateral force against slip ratio. The wheel longitudinal velocity, $w_x$, is required for calculation of wheel slip, $\lambda$. These wheel speeds take into account the lateral dynamics of the vehicle, and is calculated as

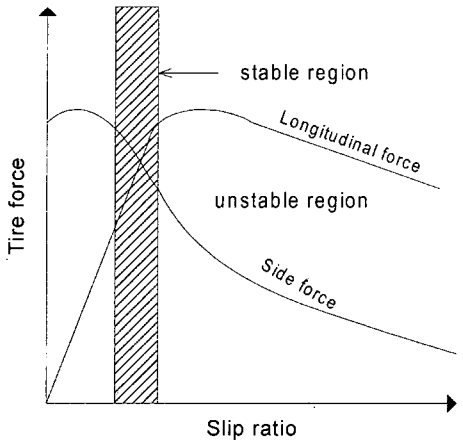


Figure 5. Wheel dynamics layout.

$$w_{fL}=\left(v_x+\frac{rT_w}{2}\right)\cos\delta+\left(v_y+\frac{rT_w}{2}\right)\sin\delta$$

$$w_{fR}=\left(v_x+\frac{rT_w}{2}\right)\cos\delta+\left(v_y+\frac{rT_w}{2}\right)\sin\delta \quad (33)$$

$$w_{rL}=v_x+\frac{rT_w}{2}$$

$$w_{rR}=v_x+\frac{rT_w}{2}$$

where $w_{fL}$, $w_{fR}$, $w_{rL}$, $w_{rR}$ are the wheel longitudinal velocities for the left front, right front, left rear and right rear wheels, respectively. $v_x$ is the vehicle longitudinal velocity, $r$ is the vehicle yaw rate, $v_y$ is the vehicle lateral velocity, $\delta$ is the front steerable road wheel angle and $T_w$ is the vehicle trackwidth. Note, for a straight-line maneuver ($\delta$=0) on a condistent surface ($r$=0), $w_x$=$v_x$, which is the typically used value in the wheel slip, $\lambda$, calculation. During the acceleration of a wheel, $w_x < \omega_r$. Hence, the wheel slip, $\lambda$, is calculated as

$$\lambda=1-\frac{w_x}{R\omega} \quad (34)$$

Differentiating equation (34) gives the derivatie form

$$\dot{\lambda}=\frac{1}{R}\left[\frac{w_x}{\omega^2}\dot{\omega}-\frac{\dot{w}_x}{\omega}\right] \quad (35)$$

Using equation (2) and equation (34), and substituting into equation (35) gives

$$\dot{\lambda}=\frac{1}{R}\left[\frac{w_x}{\omega^2}\cdot\frac{1}{I_w}(T_{wt}-RF_x-dF_z)-\frac{\dot{w}_x}{\omega}\right] \quad (36)$$

The wheel normal force, $F_z$, can be determined from the vehicle acceleration sensors and the physical vehicle parameters. The control objective is to drive the system state ($\lambda$, $\dot{\lambda}$) to the desired values ($\lambda_r$, $\dot{\lambda}_r$) by controlling the wheel torque $T_{wt}$, where $\lambda_r$ is the reference input wheel slip, and $\dot{\lambda}_r$ is the time derivative of the reference input wheel slip.

## 3. WHEEL SLIP CONTROL WITH MOVING SLIDING SURFACE FOR TCS

The main difficulty arising in the design of a wheel slip control is due to the strong nonlinearity and uncertainty in the problem. Sliding mode control is a preferable approach for this kind of problem; due to changes which always happen in working conditions, the robustness of sliding mode control is an advantage (Kazemi *et al.*, 2000).

In a vehicle, better traction performance enables better steerability and it helps the stability, too. Thus, time response of traction is important in vehicle dynamics analysis and the design parameter availability related to a response time and bounded control input constraints in a control system design should be considered for practical development.

### 3.1. Moving Sliding Surface

The required components for a sliding mode controller are a switching function, $s$, an equivalent control torque, $T_{TCS,eq}$, a striking control torque, $T_{TCS,h}$, and a continuous switching control, $T_{TCS}$. Conventionally, a switching function, $s$, is defined as

$$s=\lambda-\lambda_r \quad (37)$$

The switching function, $s$, is used by the sliding mode control to change the structure of the control law. Based on equation (37), the most common way to adjust the structure of the control law is using the sign of the switching function, sgn($s$). However, using sgn($s$) to switch between control structures can result in chattering during the sliding motion. But for robustness, control input should be increased and that makes chattering more severe and vice versa. Therefore, there is a tradeoff between robustness and chattering (Ha *et al.*, 1999).

Inspired by the works of Choi and Park (1994), Choi *et al.* (1994), and Bartoszewicz (1995), we propose time-varying tuning schemes to continuously move sliding surfaces so that fast tracking is obtained. The sliding surface slopes are determined by using an initial state and a final sliding surface for keeping sliding motion from the beginning and achieving desired sliding motion. Figure 6 shows the region for possible slopes of rotating sliding surfaces in the phase plane. Actually, to achieve the sliding mode, we multiply a slope of the rotated sliding surface to the reference input wheel slip. By this means, the representative point of the considered system is forced to stay always on our sliding surfaces. Therefore,

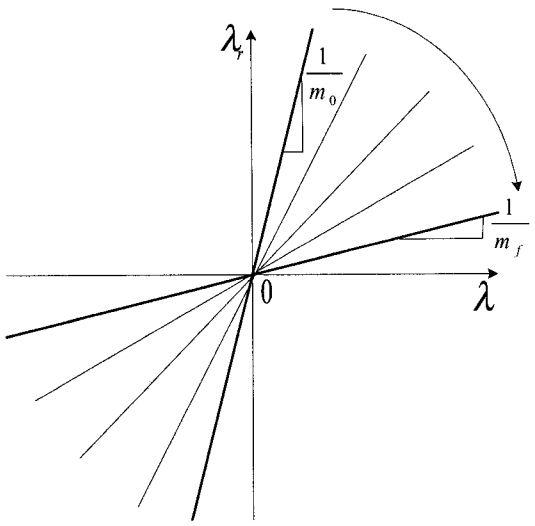


Figure 6. Rotating sliding surface ($\lambda_0 > \lambda_r$).

Table 1. Slope variation.

| Time | $m(t)$ |
|---|---|
| $t_0$ (=0) | $m_0=\lambda_0/\lambda_r$ |
| $t_f$ | $m_f \approx 1$ |

the system is truly insensitive to parameter variations and external disturbances; hence its dynamic behaviour can be precisely predetermined.

We define a switching function, $s$, as

$$s=\lambda-m(t)\lambda_r \tag{38}$$

where

$$m(t)=\left(1-\frac{\lambda_0}{\lambda_r}\right)\tanh\left(\frac{c}{t_f}t\right)+\frac{\lambda_0}{\lambda_r} \tag{39}$$

therefore $m(t)$ is the time-varying slope of the moving sliding surface, $\lambda_0$ is the wheel slip at time $t_0(=0)$, $\lambda_r$ is the reference input wheel slip, $t_f$ is the reaching time and $c$ is the design parameter. $m(t)$ is changed as follows:

Thus the sliding surface in (38) is moving as shown in Figure 6. The design parameter $c$ can be designed by the user.

As a result, from the initial state, the sliding motion occurs and the wheel slip reaches to the desired reference input wheel slip after the determined time specification, $t_f$, by keeping the sliding motion by the proposed sliding control algorithm with the moving sliding surface.

if $\lambda_0 < \lambda_r$, then the slope rotates in the increasing direction when $\frac{\lambda_0}{\lambda_r} \to 1$ ; Figure 6

if $\lambda_0 > \lambda_r$, then the slope rotates in the decreasing direction when $\frac{\lambda_0}{\lambda_r} \to 1$.

Differentiating (38), we get

$$\dot{s}=\dot{\lambda}-\dot{m}\lambda_r$$

$$=\dot{\lambda}-\left(1-\frac{\lambda_0}{\lambda_r}\right)\frac{c}{t_f}\frac{\left(\cosh^2\left(\frac{c}{t_f}t\right)-\sinh^2\left(\frac{c}{t_f}t\right)\right)}{\cosh^2\left(\frac{c}{t_f}t\right)}\lambda_r \tag{40}$$

where

$$\dot{m}=\left(1-\frac{\lambda_0}{\lambda_r}\right)\frac{c}{t_f}\frac{\left(\cosh^2\left(\frac{c}{t_f}t\right)-\sinh^2\left(\frac{c}{t_f}t\right)\right)}{\cosh^2\left(\frac{c}{t_f}t\right)} \tag{41}$$

and $t_f$ can be determined by the user and thus the design parameter related to a response time and control input in control system design is available for practical development.

### 3.2. Equivalent Control

In this section, the sliding mode controller is described to allow the wheel slip, $\lambda$, to track a reference input wheel slip, $\lambda_r$. The required components for a sliding mode controller are a switching function, $s$, an equivalent control torque, $T_{TCS,eq}$, a striking control torque, $T_{TCS,h}$, and a continuous switching control, $T_{TCS}$.

The goal of sliding mode control is to achieve a reduction in the system order dynamics, called sliding motion. This sliding motion occurs when the state ($\lambda_r$, $\dot{\lambda}_r$) reaches the sliding surface defined by $s$=0. The control that moves the state along the sliding surface is called the equivalent control. In this problem, it is called the equivalent control torque, $T_{TCS,eq}$. The dynamics of sliding motion are governed by

$$\dot{s}=0 \tag{42}$$

Differentiating equation (38), and substituting into equation (42) gives

$$\dot{\lambda}=\dot{m}\lambda_r \tag{43}$$

Using equation (40) and substituting equation (36) into equation (43) gives

$$\frac{1}{R}\left[\frac{w_x}{\omega^2}\cdot\frac{1}{I_w}(T_{TCS,eq}-RF_x-dF_z)-\frac{\dot{w}_x}{\omega}\right]=\dot{m}\lambda_r \tag{44}$$

where the equivalent control torque, $T_{TCS,eq}$, is used. Solving for the equivalent torque, $T_{TCS,eq}$, gives

$$T_{TCS,eq}=\frac{RI_w\omega^2}{w_x}\left[\dot{m}\lambda_r+\frac{\dot{w}_x}{R\omega}\right]+RF_x+dF_z \tag{45}$$

In analyzing equation (45), all variables and parameters are known, except for the wheel longitudinal acceleration, $\dot{w}_x$. A benefit to using sliding mode control is that it can handle uncertainty in the system (Khalil, 1996), as long as the bounds of the uncertainty are known. Assume that the wheel longitudinal acceleration, $\dot{w}_x$, is not known, but can be bounded by

$$\left|\dot{w}_x-\hat{\dot{w}}_x\right|\le\overline{W}_x \tag{46}$$

where $\overline{W}_x$ is the maximum wheel longitudinal acceleration. Since the wheel longitudinal acceleration, $\dot{w}_x$, is not known, it has to be replaced with its estimate, $\hat{\dot{w}}_x$, in the design. Since only an estimate is available, only an approximate equivalent torque, $\hat{T}_{TCS,eq}$, can be determined.

$$\hat{T}_{TCS,eq}=\frac{RI_w\omega^2}{w_x}\left[\dot{m}\lambda_r+\frac{\dot{w}_x}{R\omega}\right]+RF_x+dF_z \tag{47}$$

3.3. Hitting control and stability

If the system state $(\lambda, \dot{\lambda})$ is not on the sliding surface, a control term has to be added to the overall torque control signal to drive the system to the sliding surface. This additional term is called the hitting control torque, $T_{TCS,h}$, and is calculated by starting with the overall torque control, $T_{TCS}'$, equation. Define the torque control, $T_{TCS}'$ as

$$T_{TCS}'=\hat{T}_{TCS,eq}-T_{TCS,h}\mathrm{sgn}(s) \tag{48}$$

Note, when on the sliding surface ($s$=0), it is desired to have $T_{TCS,h}$=0. So, when on the sliding surface, the hitting control has no effect. However, since equation (48) contains the approximate equivalent torque, $T_{TCS,eq}$, the hitting control torque, $T_{TCS,h}$, additionally effects the system to keep the state on the sliding surface. Due to the uncertainty in the system, the state $(\lambda, \dot{\lambda})$ could stray off of the sliding surface. The hitting control torque, $T_{TCS,h}$, acts to return the state back to the sliding surface.

The hitting control torque, $T_{TCS,h}$, is determined by using the following reaching condition (49),

$$s\dot{s}\le-\eta|s| \tag{49}$$

when $\eta>0$ is a design parameter

**Theorem 1** The controller (48) is chosen as

$$T_{TCS,h}=\frac{RI_w\omega^2}{w_x}(F+\eta) \tag{50}$$

with the value for $F$ given by

$$F\ge\frac{\overline{W}_x}{R\omega} \tag{51}$$

which assumes that $\omega>0$ without loss of generosity. A vehicle with the wheel slip (34) incorporating the sliding surface (38) then satisfies the sliding condition (49).

**Proof** Let us define a Lyapunov function

$$V=\frac{1}{2}s^2 \tag{52}$$

The derivative of the Lyapujnov function can be expressed as

$$\dot{V}=s\dot{s} \tag{53}$$

Using equations (36), (40), (47), and (48), we have

$$\begin{aligned}\dot{V}&=s\dot{s}\\&=\frac{s}{R\omega}(\hat{\dot{w}}_x-\dot{w}_x)-\frac{w_x}{RI_w\omega^2}T_{TCS,h}|s|\end{aligned} \tag{54}$$

Substituting equation (50) into the equation for $\dot{V}$ then yields

$$\dot{V}=\frac{s}{R\omega}(\hat{\dot{w}}_x-\dot{w}_x)-(F+\eta)|s| \tag{55}$$

It can be shown from equation (51) that

$$\dot{V}\le-\eta|s| \tag{56}$$

so that the asymptotic stability condition (49) is satisfied. This concludes the proof.

Q.E.D

In the development of the hitting control torque, $T_{TCS,h}$, the overall torque control, $T_{TCS}'$, was assumed to have the form

$$T_{TCS}'=\hat{T}_{TCS,eq}-T_{TCS,h}\,\mathrm{sgn}(s) \tag{57}$$

With using the form specified in (48), the discontinuous switching, sgn(·), causes chattering in the control. Chattering is high frequency, finite oscillations that can result from neglecting fast dynamics, such as in actuators and sensors, in the control design process (Wellstead and Pettit, 1997). Chattering is an undesirable phenomenon where excessive wear on the actuators can occur (Edwards and Spurgeon, 1998). A solution to this issue is to replace the discontinuous switching with smooth, continuous switching, such as sat(·). Thus, the continuous switching torque control, $T_{TCS}$, has the form

$$T_{TCS}=\hat{T}_{TCS,eq}-T_{TCS,h}\mathrm{sat}\left(\frac{s}{\Phi}\right) \tag{58}$$

where $\Phi>0$ is a design parameter representing the boundary layer width around the $s$=0 sliding surface.

Table 2. Simulation parameters.

| $\lambda_r$ | $\Phi$ | $\eta$ |
|---|---|---|
| 0.1 | 0.07 | 0.5 |

## 4. SIMULATIONS

The proposed control system was simulated using Matlab/ Simulink software. The simulations include acceleration maneuvers on different road conditions. These maneuvers

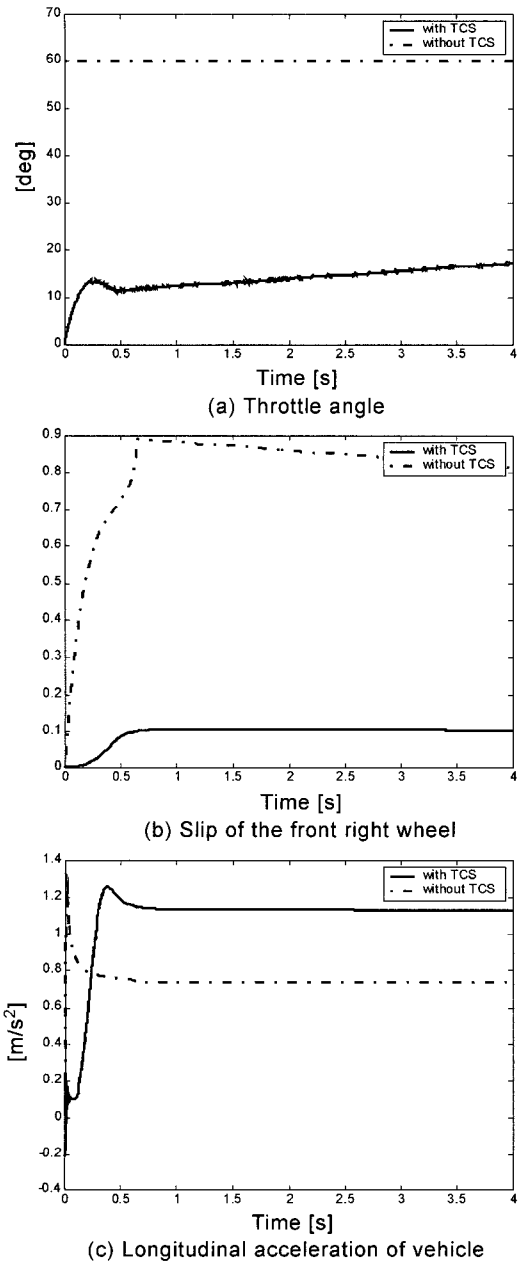


Figure 7. Simulation results for slippery road ($\mu$=0.3).

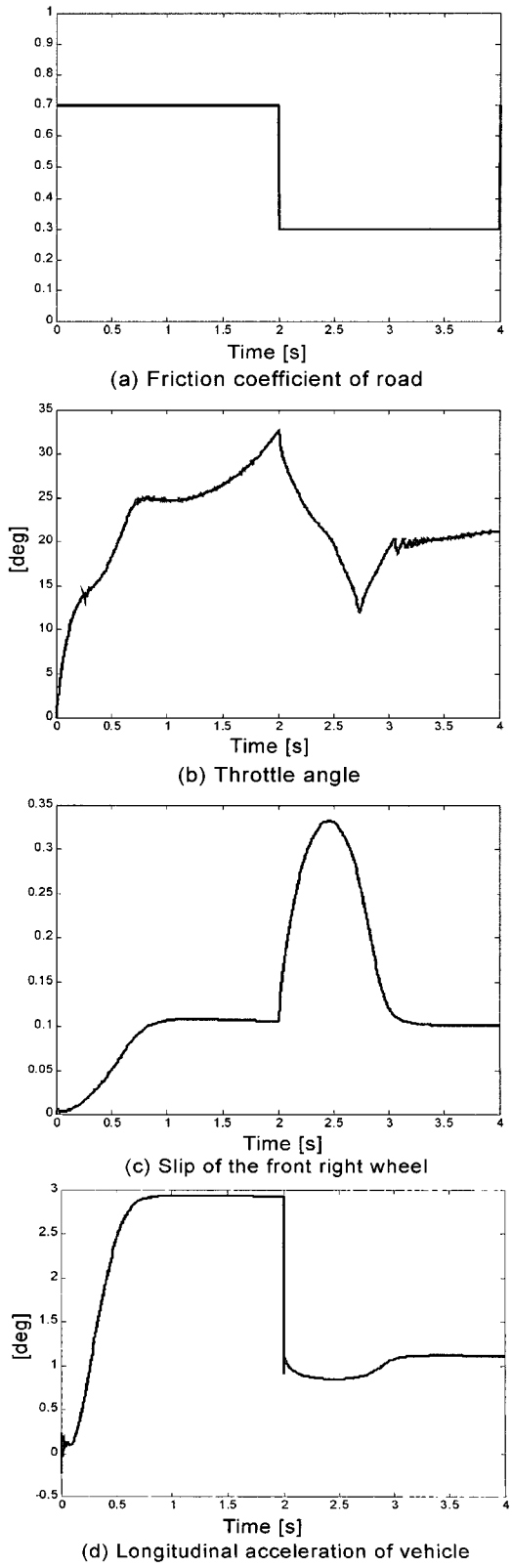


Figure 8. Simulation results for suddenly changing road condition.

considered several severe working conditions that drivers may encounter while driving. These maneuvers are:

1) Acceleration on slippery road condition;
2) Acceleration on road with suddenly changing road conditions.

The simulations performed are straight-line maneuvers ($\delta$=0), where the reference input wheel slip, $\lambda_r$, on each wheel is constant. The following tables layout the simulation parameters.

The engine torque must be controlled since the engine combustion creates the initial torque, which is transmitted through to the transmission. Hence, the engine torque is determined using the desired wheel torque and transmission ratio. In simulation, conventional sliding mode control (Slotine, 1991) is applied to control throttle angle for tracking the desired intake manifold pressure $P_{m,desired}$ computed from the wheel torque which is produced by the proposed sliding mode controller with moving sliding surface. The following sliding surface $s_e$ is used.

$$s_e=P_m-P_{m,desired} \tag{59}$$

In the first maneuver, the vehicle is accelerating on a slippery road. Results are shown in Figure 7. In order to express the significance of using of TCS especially for a slippery road ($\mu$=0.3), these results are shown with and without the traction control system. By looking at these figures, we can see that the slip of the drive wheels is controlled at a specific value. (With regard to the tire model used, the desired slip is 0.1.) As shown in Figure 7(c), longitudinal acceleration of a vehicle with TCS is better than the case without TCS.

Simulation results for the second maneuver are shown in Figure 8. Figure 8(a) shows how the suddenly changing road conditions. For this case, the desired wheel slip is 0.1 as well. Road condition changes with the effect of lower or higher wheel slip values on the system performance are negligible.

## 5. CONCLUSION

In this paper, the slip control of a vehicle is investigated. This paper focuses on the slip control through controlling the angle of the throttle valve. A 8-DOF model of the vehicle is considered along with an engine model. The controller is designed based on the notion of sliding mode control with moving sliding surface. It is simulated for various operating conditions of a vehicle during acceleration. The simulation results prove that the controller is suitable for a variety of conditions. The designed controller can be easily implemented and applied to a vehicle, as its input is a measurable one.

**Acknowledgement**–This research is supported in part by MOST (Ministry of Science and Technology) under the National Research Laboratory (NRL) grant M1-0203-00-0058-02-J00-00-031-00.

## REFERENCES

Aquino, C. F. (1981). Transient A/F control characteristics of the 5 liter central fuel injection engine. *SAE Paper No.* 810494.

Bartoszewicz, A. (1995). A comment on A time-varying sliding surface for fast and tracking control of second-order dynamic systems. *Automatica* **31**, 1893–1895.

Brunt, M. F. and Emtage, A. L. (1996). Evaluation of IMEP routines and analysis errors. *SAE Paper No.* 960609.

Choi, S. B. and Kim, J. S. (1997). A fuzzy-sliding mode controller for robust tracking of robotic manipulators. *Mechatronics* **7**, 199–216.

Choi, S. B. and Park, D. W. (1994). Moving sliding surfaces for fast tracking control of second-order dynamic systems. *ASME J. Dyn. Systems Meas. Control* **116**, 154–158.

Choi, S. B., Park, D. W. and Jayasuriya, S. (1994). A time-varying sliding surface for last and tracking control of second-order dynamic systems. *Automatica* **30**, 899–904.

Dobner, D. J. (1983). Dynamic engine models for control development part I: nonlinear and linear model formulation. *International Journal of Vehicle Design Technological Advances in Vehicle Design Series*, SP4.

Drakunov, S., Özgüner, Ü., Dix, P. and Ashrafi, B. (1995). ABS control using optimum search via sliding modes. *IEEE Transactions on Control Systems Technology* **3**, **1**, 79–85.

El Hadri, A., Cadiou, J. C., MSirdi, K. N. and Delanne, Y. (2001). Wheel-slip regulation based on sliding mode approach. *SAE* 2001 *World Congress*, USA.

Ha, Q. P., Rye, D. C. and Durrant-Whyte, H. F. (1999). Fuzzy moving sliding mode control with application to robotic manipulators. *Automatica* **34**, 607–616.

Hendricks, E. and Sorenson, S. C. (1990). Mean value modeling of spark ignition engines. *SAE Paper No.* 900616.

Kazemi, R., Kabganian, M. and Modir Zaare, M. R. (2000). A new sliding mode controller for four-wheel anti-lock braking systems (ABS). *SAE* 2000 *World Congress*, USA.

Khalil, H. K. (1996). *Nonlinear Systems, 3rd ed. Prentice-Hall*, New Jersey.

Kueon, Y. S. and Bedi, J. S. (1999). Fuzzy-neural-sliding mode controller and its applications to the vehicle anti-lock braking systems. *Proceedings of the IEEE*

*International Symposium on Industrial Electronics*, **2**, 391–398.

Landaluze, J., Mtz de Alegria, I., Auzmendi, A., Nicolás, C. F. and Reyero, R. (1999). ABS controller development based on sliding-mode theory. *American Society of Mechanical Engineers (ASME)*.

Lee, B. R. and Sin, K. H. (2000). Slip-ratio control of ABS using sliding mode control. *Proceedings of the 4th Korea-Russia International Symposium on Science and Technology*, **3**.

Moskwa, J. J. and Hedrick, J. K. (1992). Modeling and validation of automotive engines for control algorithm development. *Trans. ASME, J. Dynamic Systems, Measurement, and Control*, **114**.

Pacjeka, H. B. and Bakker, E. (1990). The magic formula tire model. *Proc. 1st Int. Colloq. Tire Models for Vehicle Dynamics Analysis*.

Powell, J. D., Fekete, N. P. and Chang, C.-F. (1998). Observer-based air-fuel ratio control. *IEEE Control Systems* **18**, **5**, 72–83.

Slotine, J.-J. E. and Li, W. (1991). *Applied Nonlinear Control*, Prentice-Hall, New Jergey.

Taylor, C. F. (1985). *The Internal Combustion Engine in Theory and Practice*, **1**, *2nd ed. MIT Press*, USA.

Yoon, P. and Sunwoo, M. (1999). A nonlinear dynamic engine modeling for controller design. *Transactions of KSAE* **7**, **7**, 167–180.

Ünsal, C. and Kachroo, P. (1999). Sliding mode measurement feedback control for antilock braking systems. *IEEE Transactions on Control Systems Technology* **7**, **2**, 271–281.